NASA/TM—2000-210215

AIAA–2000–3100

On a Self-Tuning Impact Vibration Damper for Rotating Turbomachinery

Kirsten P. Duffy
Ohio Aerospace Institute, Brook Park, Ohio

Ronald L. Bagley
University of Texas at San Antonio, San Antonio, Texas

Oral Mehmed
Glenn Research Center, Cleveland, Ohio

August 2000

The NASA STI Program Office . . . in Profile

Since its founding, NASA has been dedicated to the advancement of aeronautics and space science. The NASA Scientific and Technical Information (STI) Program Office plays a key part in helping NASA maintain this important role.

The NASA STI Program Office is operated by Langley Research Center, the Lead Center for NASA's scientific and technical information. The NASA STI Program Office provides access to the NASA STI Database, the largest collection of aeronautical and space science STI in the world. The Program Office is also NASA's institutional mechanism for disseminating the results of its research and development activities. These results are published by NASA in the NASA STI Report Series, which includes the following report types:

- TECHNICAL PUBLICATION. Reports of completed research or a major significant phase of research that present the results of NASA programs and include extensive data or theoretical analysis. Includes compilations of significant scientific and technical data and information deemed to be of continuing reference value. NASA's counterpart of peer-reviewed formal professional papers but has less stringent limitations on manuscript length and extent of graphic presentations.

- TECHNICAL MEMORANDUM. Scientific and technical findings that are preliminary or of specialized interest, e.g., quick release reports, working papers, and bibliographies that contain minimal annotation. Does not contain extensive analysis.

- CONTRACTOR REPORT. Scientific and technical findings by NASA-sponsored contractors and grantees.

- CONFERENCE PUBLICATION. Collected papers from scientific and technical conferences, symposia, seminars, or other meetings sponsored or cosponsored by NASA.

- SPECIAL PUBLICATION. Scientific, technical, or historical information from NASA programs, projects, and missions, often concerned with subjects having substantial public interest.

- TECHNICAL TRANSLATION. English-language translations of foreign scientific and technical material pertinent to NASA's mission.

Specialized services that complement the STI Program Office's diverse offerings include creating custom thesauri, building customized data bases, organizing and publishing research results . . . even providing videos.

For more information about the NASA STI Program Office, see the following:

- Access the NASA STI Program Home Page at ***http://www.sti.nasa.gov***

- E-mail your question via the Internet to help@sti.nasa.gov

- Fax your question to the NASA Access Help Desk at (301) 621-0134

- Telephone the NASA Access Help Desk at (301) 621-0390

- Write to:
  NASA Access Help Desk
  NASA Center for AeroSpace Information
  7121 Standard Drive
  Hanover, MD 21076

NASA/TM—2000-210215

AIAA–2000–3100

On a Self-Tuning Impact Vibration Damper for Rotating Turbomachinery

Kirsten P. Duffy
Ohio Aerospace Institute, Brook Park, Ohio

Ronald L. Bagley
University of Texas at San Antonio, San Antonio, Texas

Oral Mehmed
Glenn Research Center, Cleveland, Ohio

Prepared for the
Joint Propulsion Conference
sponsored by the American Institute of Aeronautics and Astronautics
Huntsville, Alabama, July 17–19, 2000

National Aeronautics and
Space Administration

Glenn Research Center

August 2000

Available from

NASA Center for Aerospace Information
7121 Standard Drive
Hanover, MD 21076
Price Code: A03

National Technical Information Service
5285 Port Royal Road
Springfield, VA 22100
Price Code: A03

Available electronically at http://gltrs.grc.nasa.gov/GLTRS

ON A SELF-TUNING IMPACT VIBRATION DAMPER FOR ROTATING TURBOMACHINERY

K. P. Duffy
Ohio Aerospace Institute
Brook Park, Ohio 44142

R. L. Bagley
University of Texas at San Antonio
San Antonio,Texas 78249

O. Mehmed
National Aeronautics and Space Administration
Glenn Research Center
Cleveland,Ohio 44135

ABSTRACT

A self-tuning impact damper is investigated analytically and experimentally as a device to inhibit vibration and increase the fatigue life of rotating components in turbomachinery. High centrifugal loads in rotors can inactivate traditional impact dampers because of friction or misalignment of the damper in the g-field. Giving an impact damper characteristics of an acceleration tuned-mass damper enables the resulting device to maintain damper mass motion and effectiveness during high-g loading. Experimental results presented here verify that this self-tuning impact damper can be designed to follow an engine order line, damping rotor component resonance crossings.

NOMENCLATURE

a	Centrifugal acceleration
A	Nondimensional amplitude – ratio of primary mass displacement amplitude to cavity clearance (C/d)
C	Primary mass displacement amplitude
d	Clearance in the damper cavity
m_1	Modal mass of the turbomachinery component (primary mass)
m_2	Mass of the self-tuning impact damper (damper mass)
N	Engine order
r	Ball radius
R	Trough radius
R_o	Distance of damper from center of rotation
t	Time
$x_1(t)$	Displacement of the primary mass
$x_2(t)$	Displacement of the damper mass relative to the primary mass
ε	Coefficient of restitution between primary and damper masses
ζ	Effective damping coefficient
$\Delta\zeta$	Damping added to the system by the damper ($\zeta-\zeta_1$)
ζ_1	Damping coefficient of the primary mass in the absence of the damper mass
ζ_2	Damping coefficient of the damper mass when the primary mass is stationary
μ	Ratio of damper mass to primary mass
ω_1	Angular frequency of the primary mass in the absence of the damper mass
ω_2	Angular frequency of the damper mass when the primary mass is stationary
ω_R	Angular velocity of the rotor

BACKGROUND

Engineers now design turbomachinery blades without shrouds, or as blisks, causing blade damping to decrease significantly because mechanical damping from shroud and blade joints is eliminated. New damping concepts are required to provide the necessary damping to avoid the problems caused by high cycle fatigue (HCF) such as cracks or even catastrophic failure. However, the engine environment precludes many existing dampers because of high temperatures and large acceleration fields. The self-tuning impact damper described here is an attempt to address the HCF problem in blades or other rotating turbomachinery components.

Self-tuning vibration absorbers have been used in the past to attenuate torsional vibrations of rotating shafts[6]. These dampers take the form of centrifugal pendulums that act as tuned-mass dampers. When the resonance frequency of the tuned mass equals the forcing frequency, the vibrations of the shaft are reduced. The self-tuning aspect of these dampers arises from the fact that their resonance frequencies are directly proportional to the rotational speed. This makes them ideal for engine blades because excitation frequencies are generally engine order, or proportional to rotor speed. Hollkamp et. al. explored the use of the centrifugal pendulum for turbomachinery blades[5]. However, adapting these dampers for blades can be problematic. First, the pendulum length may be too long for practical use in blades. Second, the thickness of a turbomachinery blade may be too small for full range of motion of a tuned-mass pendulum device.

The self-tuning impact damper was designed specifically for use in turbomachinery blades, but may also find use in other rotating components. Here, the tuned mass is a ball rolling in a spherical trough under a centrifugal load. Its natural frequency is proportional to the rotor speed, thus it has the dynamic properties of a pendulum without its length. In addition, the damper mass is expected to strike the walls of the cavity in the blade as a means of dissipating additional energy.

The self-tuning impact damper combines the characteristics of a traditional impact damper and a vibration absorber tuned by the centrifugal acceleration created by the spinning rotor. A traditional impact damper functions by dissipating energy each time its mass strikes the walls of a cavity within a harmonic oscillator, as shown in Figure 1. In a high g-field, misalignment or friction can immobilize the impactor mass. The tuned-mass damper shown in Figure 2 functions by absorbing kinetic energy from the oscillator into the tuned mass, which in turn sheds its kinetic energy through some damping mechanism. When driven at resonance, the tuned-mass damper produces maximum mass excursions within the cavity. This causes it to strike the cavity walls, thus making it an impact damper.

The self-tuning damper frequency can follow engine order lines, damping blade resonance crossings for multiple modes. For example, Figure 3 shows resonance crossings for the first bending (1B) and first torsional (1T) modes. An example of the engine-order self-tuning damper is the ball-in-trough damper shown in Figure 4. The radii of the ball and spherical trough, as well as the centrifugal acceleration, tune the damper's resonance to the frequency of excitation encountered on a speed line. The ball resonance frequency is directly proportional to the rotor speed.

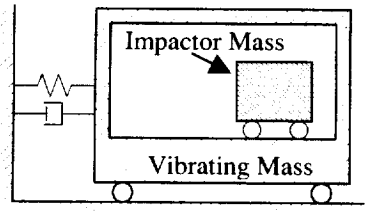

Figure 1 – Simple Impact Damper

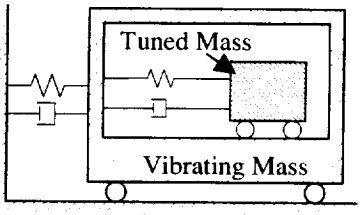

Figure 2 – Tuned-Mass Damper

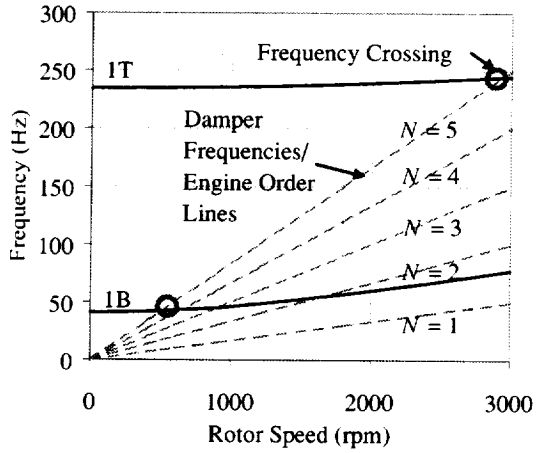

Figure 3 – Campbell Diagram

Brown and North[1] showed that the non-tuned impact damper effectiveness is a function of damper mass, coefficient of restitution, and displacement amplitude. In the current study, computer simulations of the self-tuning impact-damped harmonic oscillator were performed to determine the additional effects of damper mass frequency and viscous damping between the engine component and damper mass. For a simple tuned-mass damper, there is an optimum value of viscous damping that minimizes the resonance peak height. This study shows that an optimum damping also exists for the tuned impact damper.

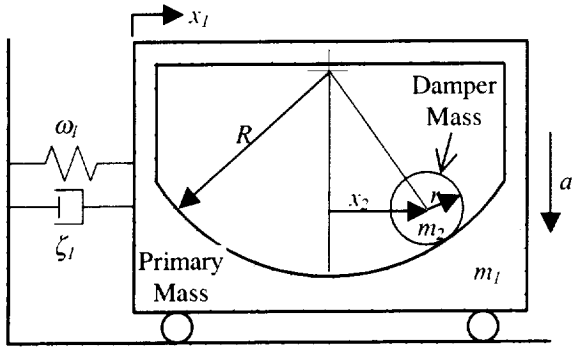

Figure 4 – Self-Tuning Impact Damper
Ball-in-Spherical-Trough Design

ANALYSIS

The damped turbomachinery component is modeled as a two-degree-of-freedom system, as shown in Figure 4. The mass-spring-damper system represents a vibration mode of the component (primary mass). A self-tuning impact damper is placed in a cavity within the primary mass.

The analysis technique follows that done by Brown and North[1]. The derivation of the equations of motion is divided into three parts. The first part describes the motion of the primary mass and damper mass between impacts. In the second part, the behavior of the system at the time of impact is characterized; impact affects the velocities of both the primary and damper masses. Finally, the damper mass can "bounce-down" against the cavity wall during a primary mass oscillation. This occurs when the damper mass makes successively smaller bounces during a primary mass half-cycle, finally coming to rest against the cavity wall. Rather than spending computational time on infinitesimally small bounces, it is assumed that the damper mass becomes stuck on the wall when the time between bounces becomes very small. The equations of motion during this time represent the primary mass and damper mass moving as one object.

MOTION BETWEEN IMPACTS

In Figure 4, the primary mass m_1 represents the modal mass of the engine component. The parameters ζ_1 and ω_1 are the damping coefficient and resonance frequency of that mode in the absence of the damper mass.

The damper mass m_2 is a ball of radius r that rolls without slip inside a spherical trough, or bowl, of radius R. The acceleration a is the radial acceleration caused by rotation. This acceleration is $a = R_o\omega_R^2$, where R_o is the distance of the ball from the center of rotation of the rotor, and ω_R is the rotor angular velocity. The primary mass displacement is $x_1(t)$, and the displacement of the ball relative to the bowl in the x-direction is $x_2(t)$.

The natural frequency of a ball rolling without slip in a trough under rotation is

$$\omega_2 = \omega_R\sqrt{\frac{5R_o}{7(R-r)}}, \tag{1}$$

assuming small displacements. Since the ball frequency is directly proportional to the rotational frequency, the ball frequency can be designed to follow an engine order N such that $\omega_2 = N\omega_R$ and

$$N = \sqrt{\frac{5R_o}{7(R-r)}}. \tag{2}$$

The equations of motion for the primary mass and the ball rolling in the bowl are

$$\left(1+\tfrac{2}{7}\mu\right)\begin{Bmatrix}\ddot{x}_1\\ \ddot{x}_2\end{Bmatrix}+\begin{bmatrix}2\zeta_1\omega_1 & -2\mu\zeta_2\omega_2\\ -\frac{5}{7}(2\zeta_1\omega_1) & 2(1+\mu)\zeta_2\omega_2\end{bmatrix}\begin{Bmatrix}\dot{x}_1\\ \dot{x}_2\end{Bmatrix}+\begin{bmatrix}\omega_1^2 & -\mu\omega_2^2\\ -\frac{5}{7}\omega_1^2 & (1+\mu)\omega_2^2\end{bmatrix}\begin{Bmatrix}x_1\\ x_2\end{Bmatrix}=\begin{Bmatrix}0\\ 0\end{Bmatrix}, \tag{3}$$

where the mass ratio is $\mu = m_2/m_1$. Here there is no external force on the system. It is assumed that there is some viscous damping between the primary mass and the damper mass, which is denoted by ζ_2. These equations differ slightly from the simple pendulum equations since the damper mass rolling effects are included.

BEHAVIOR DURING IMPACT

As the ball motion increases, it can strike the wall of the cavity. The impact behavior is modeled assuming a simple coefficient of restitution ε, and neglecting rotational inertia. Brown and North[1] show that the equations governing the behavior at impact are

$$\begin{Bmatrix}\dot{x}_1^+\\ \dot{x}_2^+\end{Bmatrix}=\begin{bmatrix}1 & \frac{\mu(1+\varepsilon)}{1+\mu}\\ 0 & -\varepsilon\end{bmatrix}\begin{Bmatrix}\dot{x}_1^-\\ \dot{x}_2^-\end{Bmatrix}, \tag{4}$$

where the superscripts $^-$ and $^+$ denote the properties immediately before and after impact, respectively.

STUCK DAMPER MASS

When the ball bounces down against the cavity wall during an oscillation, excessive computational time can be spent on infinitesimally small bounces. Thus, it is assumed that the ball becomes stuck on the wall when the time between bounces becomes very

small. The damper mass and primary mass then move as a single object. The equations describing this situation are

$$\ddot{x}_1 + \frac{2\zeta_1\omega_1}{1+\mu}\dot{x}_1 + \frac{\omega_1^2}{1+\mu}x_1 = 0,$$
$$\ddot{x}_2 = 0, \quad \dot{x}_2 = 0, \quad x_2 = \pm\frac{d}{2}, \tag{5}$$

where d is the clearance in the cavity through which the damper mass can move. These equations are invoked when the time between successive impacts falls below a specified number.

NUMERICAL ANALYSIS

Both the tuned and the impact nature of this damper were studied numerically for this simple two-degree-of-freedom system. The frequency ratio ω_2/ω_1 and the tuned mass damping ζ_2 were varied to study the effect on the effective damping coefficient ζ, which will be defined in the following section. The primary mass damping ζ_1 was set at 0.002 to agree with previous experimental data[2,3,4]. The mass ratio μ was set at 0.003, and the coefficient of restitution ε was assumed to be 0.6.

METHOD

The equations of motion governing the tuned-impact-damped system are nonlinear. Therefore, the equations were solved numerically with a FORTRAN program using an adaptable step size Runge-Kutta-Fehlberg routine.

Since the damping is a nonlinear function of primary mass amplitude, the damping was calculated from a simple free decay curve. Here, the primary mass was simulated as being released from rest from an initial displacement. The free decay displacement of the primary mass was then recorded. Figure 5 shows the free decay curve of the nondimensional displacement amplitude A as a function of time. The amplitude A is the ratio of primary mass displacement amplitude C to gap clearance d, or $A = C/d$.

A curve of the damping coefficient ζ versus the nondimensional displacement amplitude A was generated for each run, as shown in Figure 6. This was done by fitting an exponential curve $Ae^{-\zeta\omega t}$ to 25 cycles of the free decay envelope, and calculating ζ. In each case, an added damping, denoted $\Delta\zeta$, was calculated by subtracting the primary mass damping ζ_1 from the effective damping ζ. The $\Delta\zeta$ curve generally has a maximum at some displacement A_{max}. This maximum $\Delta\zeta_{max}$ is known as the peak added damping.

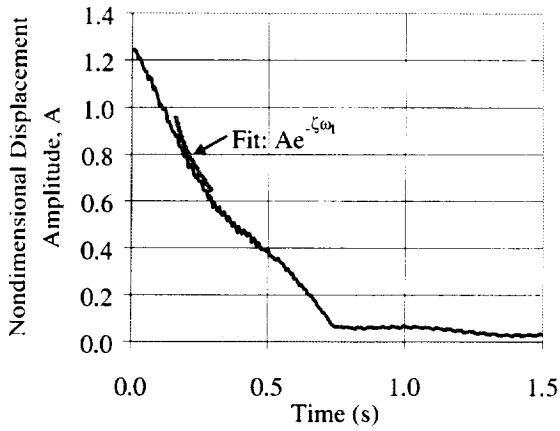

Figure 5 – Free Decay Envelope

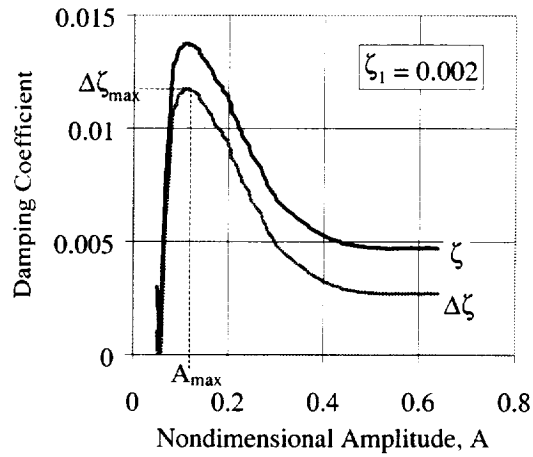

Figure 6 – Damping vs Amplitude

NUMERICAL RESULTS

Figures 7 and 8 show some numerical results for $\Delta\zeta$ for the simple tuned (non-impact) damper and $\Delta\zeta_{max}$ for the tuned impact damper, respectively. Above $\omega_2/\omega_1 = 1$, the tuned damper and the tuned impact damper perform similarly. However, when the tuned mass resonance frequency is less than the primary mass resonance frequency, or $\omega_2/\omega_1 < 1$, there is significantly more damping in the optimized tuned impact damper system. The dependence of $\Delta\zeta$ on amplitude for the self-tuning impact damper will be explored later.

Several values of ζ_2 were evaluated for both the tuned-mass and tuned-impact damped systems. Both the highest damping value and the frequency ratio at which it occurs vary with ζ_2. Figure 9 shows that for the self-tuning impact damper there is an optimum value of ζ_2 near 0.03; above and below this value the damping decreases. The frequency ratio at the highest damping approaches $\omega_2/\omega_1 = 1$ as ζ_2 increases.

Note that in Figure 9, when $\zeta_2 = 0.0$ the highest damping occurs near $\omega_2/\omega_1 = 0.8$. The ball frequency does not coincide with the primary mass frequency at that point. The engineer needs to account for the expected ζ_2 when designing the damper.

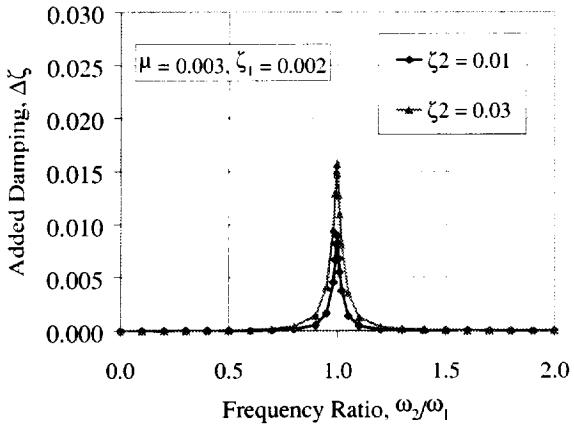

Figure 7 – Tuned-Mass Damper
Added Damping vs Frequency Ratio

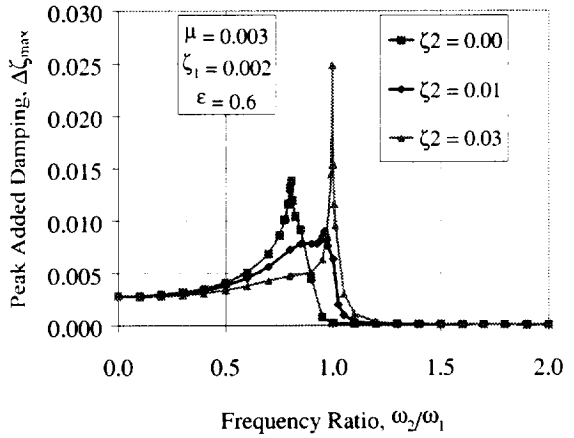

Figure 8 – Self-Tuning Impact Damper
Added Damping vs Frequency Ratio

Figure 10 shows that for the self-tuning impact damper, the nondimensional amplitude A_{max} at which the peak added damping $\Delta\zeta_{max}$ occurs also varies with frequency ratio. The amplitude A_{max} corresponding to the highest damping is very small. This is also illustrated in Figure 11. Here the added damping is shown as a function of frequency ratio for various values of A.

In order to design a damper for a specific application, the engineer needs to consult a diagram such as Figure 11. The engineer should know the expected blade displacement amplitude at the damper location, and the frequency or frequency range of interest. If large damping over a small frequency range is desired, then the damper clearance d should be chosen to give a very small A, in this case around 0.05. If damping over a larger frequency range is desired, then d should be chosen to give a moderate value of A, in this case around 0.10.

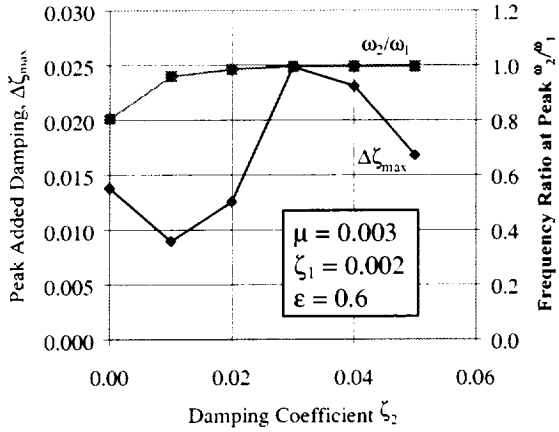

Figure 9 – Optimum Damping and Frequency Ratio
vs Damping Coefficient ζ_2

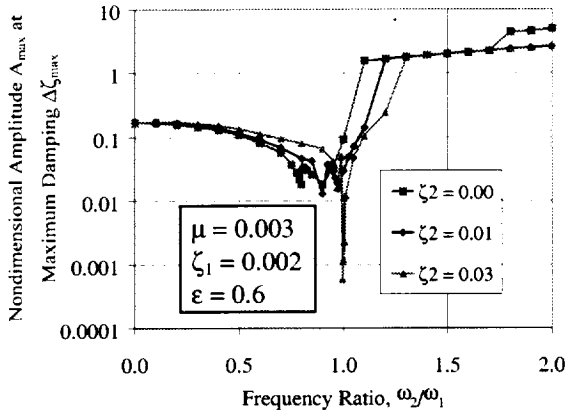

Figure 10 – Nondimensional Amplitude A at
Peak Added Damping

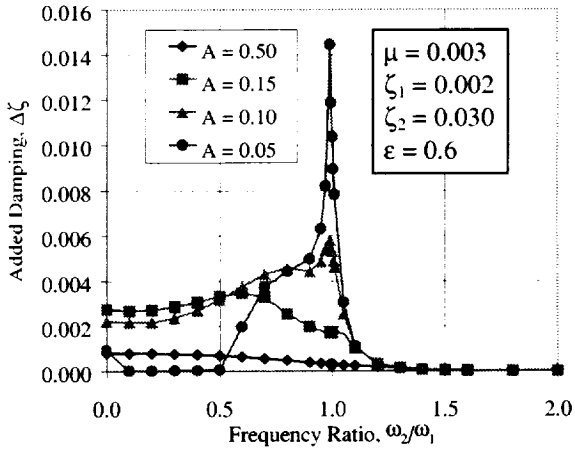

Figure 11 –$\Delta\zeta$ for Constant Nondimensional
Amplitude, A – Case: $\zeta_2 = 0.03$

EXPERIMENTAL VALIDATION

The theoretical results for free decay behavior have been validated by experiments in the Dynamic Spin Facility at NASA Glenn Research Center[2,3,4].

EXPERIMENTAL SETUP

In the spin facility shown in Figure 12, a pair of plates rotates in vacuum at up to 20,000 rpm. The rotor shaft is suspended vertically by a ball bearing at the top and a magnetic bearing at the bottom. This magnetic bearing provides excitation to the shaft causing the plates to vibrate. At a given rpm, the magnetic bearing provides a sinusoidal excitation at the plate first bending frequency (1B). The excitation is then removed and the plate vibration allowed to decay. This free decay is repeated for up to five runs at each rpm.

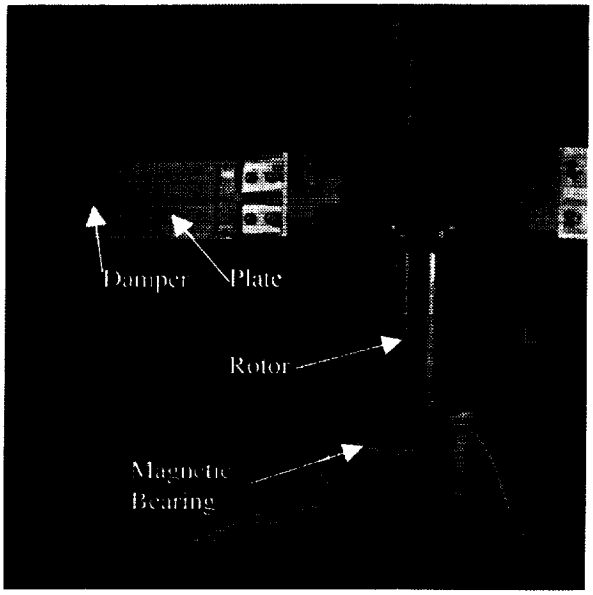

Figure 12 – Dynamic Spin Facility at NASA Glenn Research Center

Test plates are shown in Figure 13. In various experiments, two pairs of aluminum plates were tested. The plates are 3.0 inches wide, 0.063 inches thick, and either 4.0 or 6.0 inches long beyond the clamped region. They are clamped 180° apart on the rotor. There is a 0.75 inch wide by 0.75 inch long by 0.50 inch thick boss at the end of each plate that holds a damper capsule. The threaded damper capsule is 0.50 inches in diameter and 0.50 inches thick, and screws into the end of each plate. Dampers are located within the damper capsules.

Figure 13 also shows the instrumentation on the plates. There are four strain gages on each plate, two on each face at the base of the unclamped region. These gages form a bridge to give data on bending motion. There are also two accelerometers per plate, one on each inboard face of the boss. Finally, there is also a temperature gage on each plate that was not used in these tests.

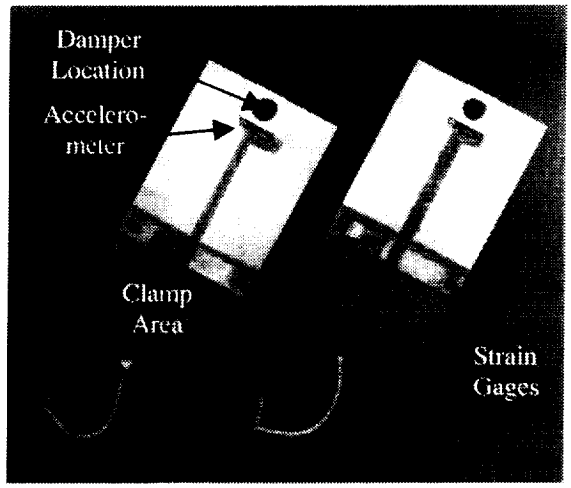

Figure 13 – Aluminum Test Plates

In Test #1, six self-tuning impact dampers, as well as one non-tuned impact damper, were tested in two pairs of rotating cantilever plates at up to 3000 rpm, or about 3100 g's. Figure 14 shows a schematic of these ball-in-trough dampers. Table 1 details the test configurations. For each configuration, a 1/8-inch diameter chrome steel ball was placed in a damping capsule. Each capsule had a hardened stainless steel bowl of a specified diameter. Each plate pair contained identical dampers for each test run. The self-tuning damper resonance frequencies followed engine order lines of $N = 3$, 4, and 5. The crossing speeds shown in Table 1 are the expected crossing speeds based on Equations 1 and 2. Figure 3 shows the Campbell diagram for the longer test plates. Test runs were also performed with undamped plates (empty damper capsules).

In Test #2, two additional ball-in-trough self-tuning impact dampers were tested in a single plate pair. The engine order of both of these dampers was near $N = 2$. The purpose of this test was to show that damping still occurs at high speeds (high centrifugal accelerations). Table 2 shows the configurations for Test #2. Again, baseline test runs were also done with undamped plates.

Note that in configuration 2-A, the engine order is non-integer ($N = 2.05$). The test system is capable of

providing excitation at any desired frequency, even a non-integer engine order.

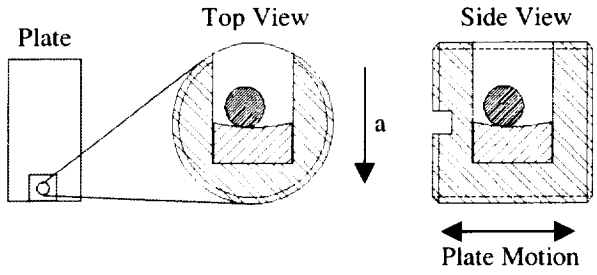

Figure 14 – Ball-in-Trough Dampers

Config-uration	Plate	Engine Order	Crossing Speed	G's at Crossing
1-A	Long	Not Tuned	Not Tuned	Not Tuned
1-B	Long	5	510 rpm	91
1-C	Long	4	655 rpm	149
1-D	Long	3	900 rpm	282
1-E	Short	5	960 rpm	268
1-F	Short	4	1375 rpm	551
1-G	Short	3	1980 rpm	1142

Table 1 – Test #1 Configurations

Config-uration	Plate	Engine Order	Crossing Speed	G's at Crossing
2-A	Short	2.05	4250 rpm	5230
2-B	Short	2.0	4890 rpm	6940

Table 2 – Test #2 Configurations

EXPERIMENTAL RESULTS

Figures 15 and 16 show the peak added damping $\Delta\zeta_{max}$ as a function of rotor speed for Test #1. Expected crossing speeds are indicated on the graphs, and are quite near to the maximum damping speeds. Again, $\Delta\zeta$ is defined as the undamped plate baseline ζ_1 subtracted from the damped plate ζ. Typically ζ_1 was approximately 0.002. Here the damping of the first bending mode was measured. The non-tuned impact dampers (configuration 1-A) were moderately successful at damping vibrations at low g's; however, their effectiveness decreased with increasing rotational speed, completely dying out by around 2000 rpm, or 1400 g's. This failure is attributed to friction and/or misalignment of the damper in the g-field. The self-tuning dampers were significantly better than the non-tuned dampers, especially near the speed line crossings when the damper resonance frequency equals the blade resonance frequency. These results are similar to the theoretical results in Figure 8.

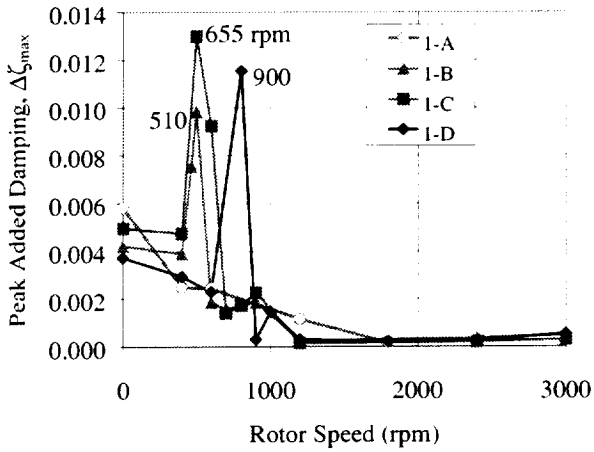

Figure 15 – Damping vs Rotor Speed Configurations 1-A – 1-D

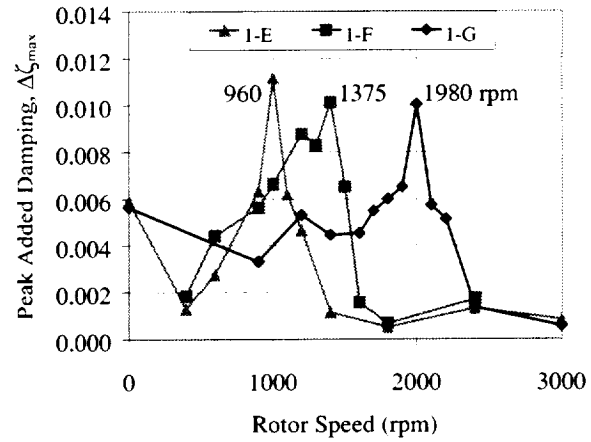

Figure 16 – Damping vs Rotor Speed Configurations 1-E – 1-G

Figure 17 shows the results from Test #2. For configuration 2-A, the peak damping did not occur near the expected crossing speed; the speed was higher than anticipated. The cause of this is currently unknown. However, significant damping was obtained at about 7250 g's, which approaches the g-levels experienced by aircraft turbomachinery blades.

The experimental results verify the preliminary theoretical results; the self-tuning impact damper is effective in reducing resonant blade response at or below speed line crossings. The results also show that the velocity of the ball near resonance overcomes friction and misalignment, causing the damper to retain effectiveness at higher g-levels.

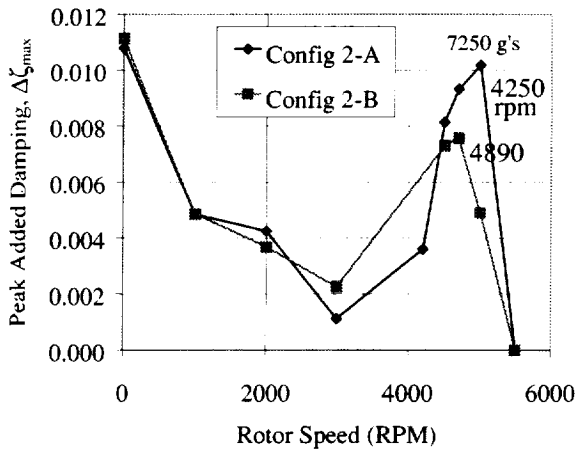

Figure 17 – Damping vs Rotor Speed
Configurations 2-A and 2-B

CONCLUSIONS

Theoretical results show that the self-tuning impact damper is a more robust design than the simple tuned damper. The tuned damper requires that the tuned mass and blade resonance frequencies be nearly identical. The self-tuning impact damper works best near the tuning frequency, but can function at a reduced level when the tuned mass resonance frequency is less than the blade resonance frequency.

Experimental results show that the self-tuning impact damper also works better than the simple impact damper in rotating blades. It has fewer problems with friction or misalignment than the non-tuned impact damper because of the spherical trough design.

Finally, both numerical and experimental results have been obtained for the unforced, free-decay case only. Since the damper is nonlinear, it is possible to have multiple solutions for a given configuration. A forced response analysis and/or test could give additional insight into how the impact damper will function in various applications.

REFERENCES

1. Brown, G.V. and North, C.M. 1987 "The Impact Damped Harmonic Oscillator in Free Decay", NASA TM 89897, ASME Vibrations Conference.
2. Duffy, K.P., Brown, G.V., and Mehmed, O. 1998 "Impact Damping of Rotating Cantilever Plates", 3rd National Turbine Engine High Cycle Fatigue Conference.
3. Duffy, K.P., Bagley, R.L., and Mehmed, O. 1999 "A Self-Tuning Impact Damper for Rotating Blades", 4th National Turbine Engine High Cycle Fatigue Conference.
4. Duffy, K.P., Bagley, R.L., and Mehmed, O. 2000 "A Self-Tuning Impact Damper for Rotating Blades", 5th National Turbine Engine High Cycle Fatigue Conference.
5. Hollkamp, J.J., Bagley, R.L., and Gordon, R.W. 1999 "A Centrifugal Pendulum Absorber for Rotating, Hollow Engine Blades", Journal of Sound and Vibration, v. 219 n. 3, pp. 539-549.
6. Sharif-Bakhtar, M. and Shaw, S.W. 1988 "The Dynamic Response of a Centrifugal Pendulum Vibration Absorber with Motion-Limiting Stops," Journal of Sound and Vibration, v. 126 n. 2, pp. 221-235.

REPORT DOCUMENTATION PAGE

Form Approved
OMB No. 0704-0188

1. AGENCY USE ONLY (Leave blank)	2. REPORT DATE	3. REPORT TYPE AND DATES COVERED
	August 2000	Technical Memorandum

4. TITLE AND SUBTITLE

On a Self-Tuning Impact Vibration Damper for Rotating Turbomachinery

5. FUNDING NUMBERS

WU-274-00-00-00

6. AUTHOR(S)

Kirsten P. Duffy, Ronald L. Bagley, and Oral Mehmed

7. PERFORMING ORGANIZATION NAME(S) AND ADDRESS(ES)

National Aeronautics and Space Administration
John H. Glenn Research Center at Lewis Field
Cleveland, Ohio 44135-3191

8. PERFORMING ORGANIZATION REPORT NUMBER

E-12334

9. SPONSORING/MONITORING AGENCY NAME(S) AND ADDRESS(ES)

National Aeronautics and Space Administration
Washington, DC 20546-0001

10. SPONSORING/MONITORING AGENCY REPORT NUMBER

NASA TM—2000-210215

11. SUPPLEMENTARY NOTES

Prepared for the Joint Propulsion Conference sponsored by the American Institute of Aeronautics and Astronautics, Huntsville, Alabama, July 17–19, 2000. Kirsten P. Duffy, Ohio Aerospace Institute, 22800 Cedar Point Road, Brook Park, Ohio 44142 (work funded under NASA Cooperative Agreement NCC3–724); Ronald L. Bagley, Associate Professor, University of Texas at San Antonio, San Antonio, Texas 78249–1130; and Oral Mehmed, Senior Research Engineer, NASA Glenn Research Center. Responsible person, Ben Choi, organization code 5930, (216) 433–6040.

12a. DISTRIBUTION/AVAILABILITY STATEMENT

Unclassified - Unlimited
Subject Categories: 07 and 39 Distribution: Nonstandard

This publication is available from the NASA Center for AeroSpace Information, (301) 621–0390.

12b. DISTRIBUTION CODE

13. ABSTRACT ***(Maximum 200 words)***

A self-tuning impact damper is investigated analytically and experimentally as a device to inhibit vibration and increase the fatigue life of rotating components in turbomachinery. High centrifugal loads in rotors can inactivate traditional impact dampers because of friction or misalignment of the damper in the g-field. Giving an impact damper characteristics of an acceleration tuned-mass damper enables the resulting device to maintain damper mass motion and effectiveness during high-g loading. Experimental results presented here verify that this self-tuning impact damper can be designed to follow an engine order line, damping rotor component resonance crossings.

14. SUBJECT TERMS

Turbomachine blades; Vibration damping; Spin tests

15. NUMBER OF PAGES

14

16. PRICE CODE

A03

17. SECURITY CLASSIFICATION OF REPORT	18. SECURITY CLASSIFICATION OF THIS PAGE	19. SECURITY CLASSIFICATION OF ABSTRACT	20. LIMITATION OF ABSTRACT
Unclassified	Unclassified	Unclassified	